THE JOURNAL OF BIOLOGICAL CHEMISTRY VOL. 292, NO. 9, pp. 3624–3636, March 3, 2017

Ectopic Expression of Mouse Melanopsin in *Drosophila* Photoreceptors Reveals Fast Response Kinetics and Persistent Dark Excitation*

Received for publication, August 21, 2016, and in revised form, January 19, 2017 Published, JBC Papers in Press, January 24, 2017, DOI 10.1074/jbc.M116.754770

Bushra Yasin[‡], Elkana Kohn[‡], Maximilian Peters[‡], Rachel Zaguri[‡], Shirley Weiss[‡], Krystina Schopf[§], Ben Katz[‡], Armin Huber[§], and Baruch Minke[‡1]

From the [‡]Department of Medical Neurobiology, Institute for Medical Research Israel-Canada (IMRIC) and the Edmond and Lily Safra Center for Brain Sciences (ELSC), Faculty of Medicine, Hebrew University, Jerusalem 91120, Israel and the [§]Department of Biosensorics, Institute of Physiology, University of Hohenheim, 70599 Stuttgart, Germany

Edited by Henrik G. Dohlman

The intrinsically photosensitive M1 retinal ganglion cells (ipRGC) initiate non-image-forming light-dependent activities and express the melanopsin (OPN4) photopigment. Several features of ipRGC photosensitivity are characteristic of fly photoreceptors. However, the light response kinetics of ipRGC is much slower due to unknown reasons. Here we used transgenic *Drosophila*, in which the mouse OPN4 replaced the native Rh1 photopigment of *Drosophila* R1–6 photoreceptors, resulting in deformed rhabdomeric structure. Immunocytochemistry revealed OPN4 expression at the base of the rhabdomeres, mainly at the rhabdomeral stalk. Measurements of the early receptor current, a linear manifestation of photopigment activation, indicated large expression of OPN4 in the plasma membrane. Comparing the early receptor current amplitude and action spectra between WT and the Opn4-expressing *Drosophila* further indicated that large quantities of a blue absorbing photopigment were expressed, having a dark stable blue intermediate state. Strikingly, the light-induced current of the Opn4-expressing fly photoreceptors was ~40-fold faster than that of ipRGC. Furthermore, an intense white flash induced a small amplitude prolonged dark current composed of discrete unitary currents similar to the *Drosophila* single photon responses. The induction of prolonged dark currents by intense blue light could be suppressed by a following intense green light, suggesting induction and suppression of prolonged depolarizing afterpotential. This is the first demonstration of heterologous functional expression of mammalian OPN4 in the genetically emendable *Drosophila* photoreceptors. Moreover, the fast OPN4-activated ionic current of *Drosophila* photoreceptors relative to that of mouse ipRGC, indicates that the slow light response of ipRGC does not arise from an intrinsic property of melanopsin.

The intrinsically photosensitive retinal ganglion cells (ipRGC)[2] are a subclass of retinal ganglion cells expressing the visual pigment, melanopsin (OPN4), which calibrates by direct photic input the circadian pacemaker of the master circadian clock and supports some non-image forming light-dependent functions (reviewed in Ref. 1). There are difficulties in advancing understanding of ipRGC phototransduction. The main obstacle is the scarcity of ipRGC and the low expression levels of phototransduction proteins in these cells. This difficulty makes it nearly impossible to investigate phototransduction of the ipRGC by employing the same set of biochemical and electrophysiological approaches that proved successful in characterizing rhodopsin signaling processes in image-forming rod photoreceptor cells. Therefore, at present, the knowledge of phototransduction of ipRGC is still fragmented (1). A promising way to characterize the OPN4 photopigment arises from the apparent similarity between phototransduction of ipRGC and invertebrates. It has been well established that several features of ipRGC photosensitivity are also characteristic of invertebrate photoreceptor cells. (i) OPN4 shares more sequence similarity with invertebrate rhodopsins than with vertebrate rhodopsins (2). (ii) ipRGC depolarize upon light activation like invertebrate photoreceptors (3–5). (iii) Photoactivation causes a transient increase in cytosolic Ca^{2+} levels (6), and the photocurrent generated by ipRGC exhibits a current-voltage relationship that resembles that of the TRPC channels (7, 8), which are the light-activated channels of *Drosophila* photoreceptor cells (9, 10). (iv) Similar to *Drosophila* photoreceptor cells, the ipRGC express G_q/G_{11} and PLCβ4 (11–13), and the OPN4-mediated photocurrent in ipRGC can be blocked by specific inhibitors of G_q/G_{11} and PLCβ proteins (11). In the PLC$\beta4^{-/-}$ KO mice, in addition to removing the intrinsic pupillary light reflex, OPN4 activity was also eliminated in M1-ipRGC (13).

OPN4 uses 11-*cis*-retinaldehyde as a chromophore (14), which upon photon absorption photoisomerizes to all-*trans*-retinal, forming a dark stable meta (M) state, which activates the downstream signaling proteins. There are indications that,

* This work was supported by grants from the Israel Science Foundation (ISF), the Deutsch-Israelische Projektkooperation (DIP), and the US-Israel Binational Science Foundation (BSF). The authors declare that they have no conflicts of interest with the contents of this article.

[1] To whom correspondence should be addressed: Dept. of Medical Neurobiology, Faculty of Medicine, Hebrew University, Jerusalem 91120, Israel. Tel.: 972-2-6758407; Fax: 972-2-6439736; E-mail: baruchm@ekmd.huji.ac.il.

[2] The abbreviations used are: ipRGC, intrinsically photosensitive retinal ganglion cell(s); ERC, early receptor current; PDA, prolonged depolarizing afterpotential; LIC, light-induced current; TRP, transient receptor potential; PLC, phospholipase C; EM, electron micrograph.

similar to invertebrate rhabdomeric photopigments, OPN4 has a dark stable M state (metamelanopsin) that can be photoregenerated by illuminating its 11-*cis* R state (5, 15, 16). Purified OPN4 from amphioxus (a marine chordate) showed a bistable photopigment with peak absorption of the R state at 485 nm and a slightly red-shifted M state with peak absorption at ~510 nm (17).

Spectrophotometric studies on expressed mouse OPN4 revealed an additional dark stable state of OPN4 with the 7-*cis* configuration, designated extramelanopsin, which can be photoconverted to OPN4 M state by blue light (15). Recent studies showed that both the 7-*cis* and the 11-*cis* physiologically "silent" OPN4 photopigment states become physiologically active when photoconverted to the active all-*trans* M state. Thus, the functional melanopsin tristability is useful for maintained photopigment availability for sustained signaling and promotes uniform activation across wavelength (5). Previous indirect experiments on heterologously expressed mammalian OPN4s have also suggested a bistable nature of OPN4 (18–20). In contrast, the M state of vertebrate rods and cones is unstable, resulting in the dissociation of the chromophore from the opsin at physiological temperatures. Like OPN4 but unlike rods/cones, *Drosophila* M state is dark stable and can be photoisomerized to the basal rhodopsin state (reviewed in Refs. 21 and 22). All of these observations indicate that OPN4 employs a downstream signaling scheme similar to that of *Drosophila* phototransduction, which is distinct from the cilliary visual pigment signaling pathway.

Mouse OPN4 was previously expressed in *Drosophila* R1–6 photoreceptor cells (23). This study apparently indicated that no functional expression of OPN4 took place in R1–6 cells. This is because there was no electroretinogram (ERG) response to light in transgenic flies expressing OPN4, in which the native Rh1 photopigment was eliminated by the null $ninaE^{I17}$ mutation. However, rhodopsin has dual functions: (i) it initiates the generation of the light response, and (ii) it is required for maintaining the structure of the signaling compartment, the rhabdomere. These two functions can be separated experimentally. Indeed, it was shown that ectopic expression of bovine rhodopsin in *Drosophila* R1–6 cells on $ninaE^{I17}$ null Rh1 background rescued the structure of the rhabdomeres without restoring the ERG response to light (24).

The slow physiological light response of ipRGC expressing melanopsin (a rise time of several seconds and duration of ~50 s in mice) is a well documented phenomenon with many implications, which has been attributed to an intrinsic property of melanopsin (25). This claim is consistent with the heterologous expression of melanopsin-producing responses that are similar across cell types, and differing as one would expect for different melanopsins (26, 27). The melanopsin-containing photoreceptors of amphioxus produce fast light responses (28). However, amphioxus melanopsin belongs to a different family from the mammalian melanopsins (29).

In the present work, we have studied ectopically expressed mouse OPN4 in *Drosophila* R1–6 photoreceptors, in which the native Rh1 photopigment was removed genetically. This study demonstrates, for the first time, heterologous functional expression of mammalian OPN4 in large quantities in the genetically emendable and easy to manipulate *Drosophila.* We showed that the functionally expressed OPN4 in the *Drosophila* photoreceptors generated a light-induced current, which is ~40-fold faster relative to that of mouse ipRGC. This result indicates that the slow light response of ipRGC does not arise from an intrinsic property of melanopsin.

Results

Expression of Melanopsin in Transgenic Drosophila Lacking the Native Photopigment—The apparent close similarity between phototransduction of *Drosophila* and ipRGC has led a number of investigators to express mammalian OPN4 in *Drosophila* photoreceptors. However, they failed to observe functional expression of OPN4 in adult flies (23, 30). This failure, most likely, resulted from the use of the insensitive ERG signal to monitor functional expression of OPN4 (*e.g.* see supplemental Fig. S8 in Ref. 23). Monitoring OPN4-induced light response in transgenic *Drosophila* photoreceptors can be a major step toward studying OPN4 properties. This is because it would establish an effective expression system to study melanopsin, and it would allow monitoring possible interactions of OPN4 with the thoroughly investigated signaling proteins of *Drosophila* photoreceptors (21). Such interactions may shed light on the properties of OPN4 in comparison with fly photopigment.

Characterization of Transgenic Drosophila Flies Expressing Mouse Opn4—To examine the possibility of functional expression of OPN4 in *Drosophila* photoreceptors, we studied ectopically expressed mouse OPN4 in the *Drosophila* R1–6 photoreceptor cells. This transgenic fly should express OPN4 exclusively in *Drosophila* R1–6 cells driven by the ninaE (Rh1) promoter on $ninaE^{I17}$ null mutant background (P[Rh1:OPN4]; $ninaE^{I17}$, hereafter abbreviated as *opn4*;$ninaE^{I17}$). To confirm the expression of the OPN4 in the transgenic fly, we isolated RNA from WT, $ninaE^{I17}$, and *opn4*;$ninaE^{I17}$ fly heads and created a cDNA library by RT-PCR using poly(A) primer. Using specific *Opn4* primers (see "Experimental Procedures"), we performed a PCR on WT, $ninaE^{I17}$, and *opn4*;$ninaE^{I17}$ cDNA libraries and, as a positive control, a plasmid containing the mouse OPN4. A PCR product of the correct size was observed for *opn4*;$ninaE^{I17}$ and the OPN4 plasmid, whereas no product was observed in WT or $ninaE^{I17}$ (Fig. 1*A*, *right lanes*). In the control experiments, we used a set of *pinta* primers (primers of the fly retinal protein designated "prolonged depolarization after-potential is not apparent" (31)). A PCR product of the correct size was observed for WT, $ninaE^{I17}$, and *opn4*;$ninaE^{I17}$, but not for the OPN4 plasmid (Fig. 1*A*, *left lanes*).

In the $ninaE^{I17}$ *Drosophila* mutant lacking the Rh1 photopigment, the signaling compartment (the rhabdomere) is highly reduced in size at eclosion, as can be seen by an electron micrograph (EM) cross-section (Fig. 1*B*, *middle*). In the *opn4*;$ninaE^{I17}$ flies, although the rhabdomeres were also reduced in size at eclosion, the rhabdomeres were larger relative to the $ninaE^{I17}$ mutant (Fig. 1*B*, *right*), but they were still smaller relative to the rhabdomeres of WT flies (Fig. 1*B*, *left*), showing deformed structure. Nevertheless, the increase in rhabdomere diameter in *opn4*;$ninaE^{I17}$ flies relative to the $ninaE^{I17}$ mutant indicates some rescue of the rhabdomeral size and shape

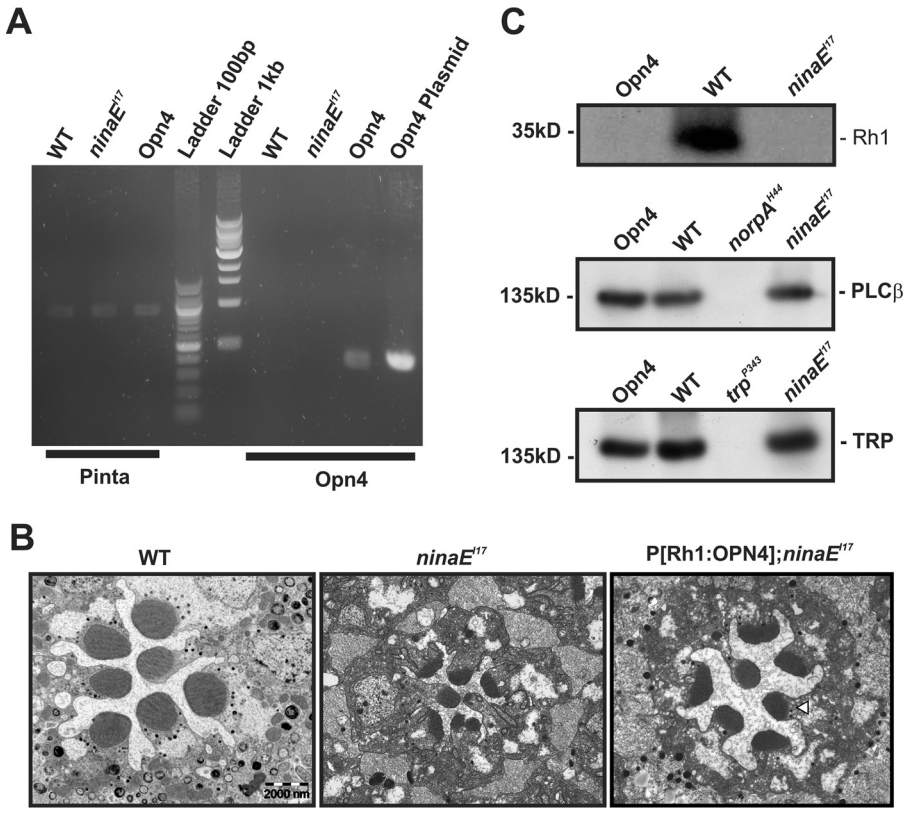

FIGURE 1. **Characterization of *Drosophila* transgene expressing mouse melanopsin (OPN4).** *A*, *Opn4* mRNA was detected in P[Rh1:OPN4];*ninaE*^{I17} transgenic flies. RT-PCR analysis, using primers of *Opn4*, showed expression of *Opn4* mRNA (predicted size, 356 bp) in fly heads of *opn4*;*ninaE*^{I17} transgenic flies but not in the heads of WT or *ninaE*^{I17} mutant flies. An OPN4 plasmid was used as a positive control for the *Opn4* primers. Primers for *pinta* ("prolonged depolarization after-potential is not apparent" (31); predicted size, 878 bp) were used as a positive control for cDNA synthesis. The *middle lanes* show the 100-bp and 1-kb ladder. The presented RT-PCR represents four independent experiments. *B*, expression of OPN4 partially rescued *ninaE*^{I17} retinal structural deformation. Representative EM of freshly eclosed *opn4*;*ninaE*^{I17} retina showing partial prevention of shrinkage of their rhabdomeres relative to *ninaE*^{I17} mutant and WT flies. Thin EM sections of ommatidia from *ninaE*^{I17} mutant (*middle column*), WT (*left column*), and *opn4*;*ninaE*^{I17} transgenic flies (*right column*) are shown. The *white arrowhead* indicates the location of the rhabdomeral stalk in which OPN4 is localized (see Fig. 2). *Scale bar*, 2 μm for all *panels*. *C*, Western blotting analysis showing no expression of Rh1 photopigment in *opn4*;*ninaE*^{I17} and *ninaE*^{I17} heads but normal expression of PLCβ and TRP. *Top*, Rh1 appeared only in WT and not in *opn4*;*ninaE*^{I17} and *ninaE*^{I17} flies. *Middle*, normal level of PLCβ appeared in *opn4*;*ninaE*^{I17} and *ninaE*^{I17} flies but not in the *norpA*^{H44} null PLCβ mutant (40) (negative control). *Bottom*, normal level of the TRP channel appeared in *opn4*;*ninaE*^{I17} and *ninaE*^{I17} flies but not in the *trp*^{P343} null mutant (67) (negative control). The labeling intensity of αRh1, $\alpha G_q\alpha$, αPLCβ, αTRP, αTRPL, and αdMoesin (protein loading control; see "Experimental Procedures") was compared between WT, *opn4*;*ninaE*^{I17}, and *ninaE*^{I17} ($n = 3$). The figure shows expression levels of several signaling proteins, which have strong effects on the *Drosophila* LIC when their expression levels are reduced (*i.e.* $G_q\alpha$ is not presented because its level has to be reduced to $<$30% of normal to have a detectable effect on the LIC (50).

by OPN4 expression, as reported previously for ectopically expressed human melanopsin in *Drosophila* R1–6 cells (30).

To directly demonstrate expression and cellular localization of OPN4 in *Drosophila* photoreceptors, we applied immunocytochemistry using a mouse anti-OPN4 antibody (α-melanopsin). To accurately localize expression of OPN4 with relation to the rhabdomeres, we also used fluorescently labeled phalloidin, which marks the actin cytoskeleton of the rhabdomeres. In agreement with the EM picture of the *opn4*;*ninaE*^{I17} ommatidium, showing deformed rhabdomeric structure (Fig. 1*B*), the phalloidin labeling revealed abnormal actin localization and weak actin staining of rhabdomeres relative to WT (Oregon R, Fig. 2, *bottom*). Nevertheless, a clear marking of smaller than normal rhabdomeres was observed (Fig. 2, *top* and *middle rows*). Importantly, an OPN4-specific staining was observed, which was confined mainly to the rhabdomeral stalk, but also to the base of the rhabdomeres of *opn4*;*ninaE*^{I17} ommatidia (Fig. 2, *top*, *merge*, *arrowhead*). This result directly demonstrated expression of mouse OPN4 adjacent to the rhabdomeric region.

We also examined by Western blotting analysis the expression levels of the major signaling proteins, Rh1, $G_q\alpha$, PLCβ, TRP, and TRPL, in *opn4*;*ninaE*^{I17} fly heads relative to heads of WT flies. The Western blotting analyses revealed that except for Rh1, which was missing in *opn4*;*ninaE*^{I17} fly heads (because of the *ninaE*^{I17} mutant background; see Fig. 1*C*), similar expression levels of $G_q\alpha$, PLCβ, TRP, and TRPL were observed in both WT and the *opn4*;*ninaE*^{I17} flies (see examples for PLCβ and TRP in Fig. 1*C*).

Induction of a Fast Photocurrent in R1–6 Cells of opn4;ninaE^{I17} *Flies Suggests Large Expression of OPN4 in the Plasma Membrane*—To validate expression of OPN4 in the plasma membrane of *opn4*;*ninaE*^{I17} photoreceptor cells and to estimate the amount of its surface membrane expression, we used the early receptor current (ERC), as a monitor of photopigment expression in the surface membrane. The ERC is a reliable electrical monitor of photopigment expression (28), even in physiologically non-responsive photoreceptor cells (32, 33). The ERC (called early receptor potential when voltage is measured (32)) is a well characterized direct electrical manifestation of conformational changes of photopigments induced by intense lights (34). It arises from redistribution of charges during conformational changes of the photopigment upon intense light

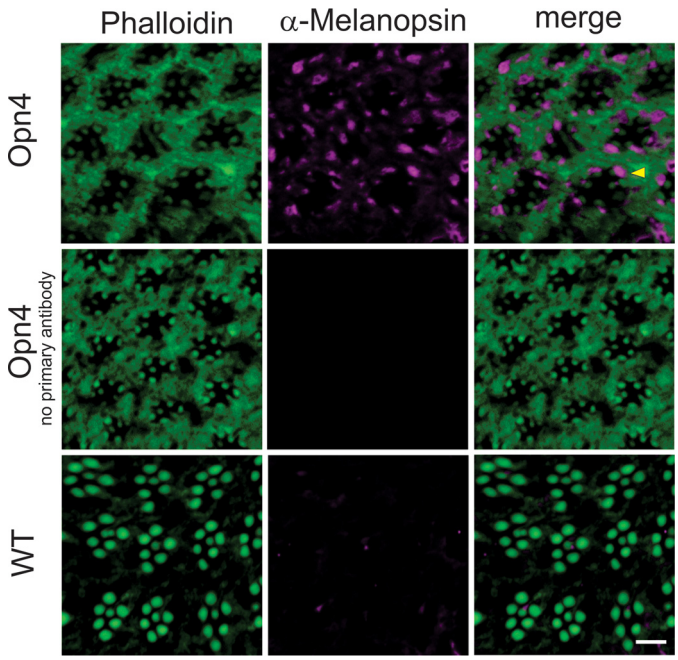

FIGURE 2. **Immunocytochemical localization of OPN4 in photoreceptors of P[Rh1:OPN4];*ninaE*^{I17} transgenic flies.** Cross-sections through the eyes of freshly eclosed P[Rh1:Opn4];*ninaE*^{I17} transgenic flies and wild type (WT, Oregon R). Sections were incubated with an α-OPN4 antibody (*purple*), except for the negative control without primary antibody, and with phalloidin (*green*), which labels actin. An *overlay* of *both colors* in the *merged panels* appears in *purple*, *green*, and *light purple* at the base of some rhabdomeres. The *yellow arrowhead* indicates the location of the rhabdomeral stalk in which OPN4 is localized (*purple*). *Scale bar*, 5 μm.

stimulation (35). When using whole cell recordings from isolated *opn4*;*ninaE*^{I17} ommatidia, intense blue flash stimulation induced a fast biphasic current with submicrosecond latency (Fig. 3*A*, *red trace*).

To examine whether the observed fast electrical signal is indeed an ERC, we also performed the experiment on the *ninaE*^{I17} null Rh1 mutant under identical illumination conditions (Fig. 3*B*, *black trace*). We did not observe any ERC signal, as reported previously (33), thus supporting the notion that the signal observed in the *opn4*;*ninaE*^{I17} is an ERC. In addition, the lack of any detectable current in whole cell recordings from R1–6 cells of *ninaE*^{I17} isolated ommatidia, in response to intense lights, indicated that the robust light response of the intact central R7,8 cells of these ommatidia did not contaminate our recordings.

It has been well established that the expression of photopigments is highly dependent on the level of retinoids in the eye. Accordingly, a retinoid-deficient diet resulted in highly reduced photopigment levels (36). To further substantiate that the observed electrical signal of the *opn4*;*ninaE*^{I17} photoreceptor cells originated from the OPN4 photopigment and constituted an OPN4-induced ERC signal, we raised *opn4*;*ninaE*^{I17} flies on a medium without retinoids, which are required for photopigment synthesis (37, 38). We found that flies raised on retinoid-deficient medium for 3 generations did not generate a detectable ERC in response to the same intense blue light (Fig. 3, *A* (*black trace*) and *D*). This observation strongly suggests that the biphasic ERCs in *opn4*;*ninaE*^{I17} photoreceptor cells arise from robust expression of a retinoid-dependent photopigment, most likely OPN4 (see below).

To further establish the use of the ERC as a reliable monitor of photopigment expression in the plasma membrane, we characterized the ERC of WT *Drosophila* photopigment, Rh1, (which encodes by the *ninaE* gene) under experimental conditions identical to those used for measuring the ERC of *opn4*;*ninaE*^{I17} photoreceptors. In voltage clamp current measurements by whole cell recordings of the ERC, activation of the rhodopsin (3OH-11-*cis*, R state, peak absorption at ~490 nm) elicited a positive ERC, whereas activation of its dark stable intermediate metarhodopsin (3OH-all-*trans*, M state, peak absorption at ~580 nm (39)) elicited a negative ERC (33). A reversed polarity was obtained previously in intracellular voltage recordings (32, 40). We found that blue light activation of WT *Drosophila* M and R states induced a biphasic negative and positive ERC current, respectively (Fig. 3*B*, *red trace*), whereas the ERC signal was absent in the *ninaE*^{I17} mutant (Fig. 3*B*, *black trace*). These results are consistent with the notion that the ERC arises from activation of the Rh1 photopigment in WT R1–6 photoreceptor cells (Fig. 3*B*). In addition, in WT photoreceptors, an intense orange light, which is maximally absorbed by the Rh1 M state, but not by its R state, elicited a pure negative ERC (Fig. 3*C*, *red*). Thus, the observed biphasic ERC of the *opn4*;*ninaE*^{I17} fly (Fig. 3*A*) with a waveform similar to that of WT photoreceptor cells but of 2.21-fold smaller average negative response amplitude (to intense blue flash; Fig. 3*D*) indicated a relatively large OPN4 expression in these transgenic flies (see "Discussion").

The Expressed OPN4 Revealed a Photopigment with Blue Absorbing R and M States—To further support the use of the ERC as a monitor of OPN4 expression in the plasma membrane, we measured the action spectra of OPN4 R and M pigment states using the ERC. As a control for these measurements, we examined whether the ERC amplitude of *opn4*;*ninaE*^{I17} flies increased linearly with the increased intensity of flash light stimuli. To this end, the average peak amplitude of the negative phase of the ERC was plotted as a function of the relative light intensity in log-log scale (Fig. 4). The experimental points were well fitted ($R^2 = 0.99$) with a linear regression curve showing linearity. As an additional control for the measurements of OPN4 action spectra, we measured the action spectra of the well characterized native *Drosophila* Rh1 R and M pigment states in WT flies using the ERC signal. The action spectrum of the positive ERC measured in WT photoreceptor cells revealed a blue-green photopigment peaking at ~490 nm with high UV sensitivity, typical for WT *Drosophila* Rh1 R state (Fig. 5*A*, *blue*). The UV sensitivity arises from a sensitizing pigment (peak sensitivity ~380 nm (41)). The action spectrum of the negative ERC revealed a photopigment state peaking in the orange range (~580 nm), typical for the Rh1-M state (Fig. 5*A*, *red*). Establishing the whole cell recorded ERC as a reliable measure of Rh1 R and M spectra allowed us to use the biphasic ERC for measuring the action spectra of OPN4 pigment states using the same light source and color filters used for WT flies (see Table 1). Unlike the ERC arising from activation of Rh1 (Fig. 3, *B* and *C*), the ERC of OPN4-expressing flies remained biphasic at all tested wavelengths from UV up to green-orange (546 nm;

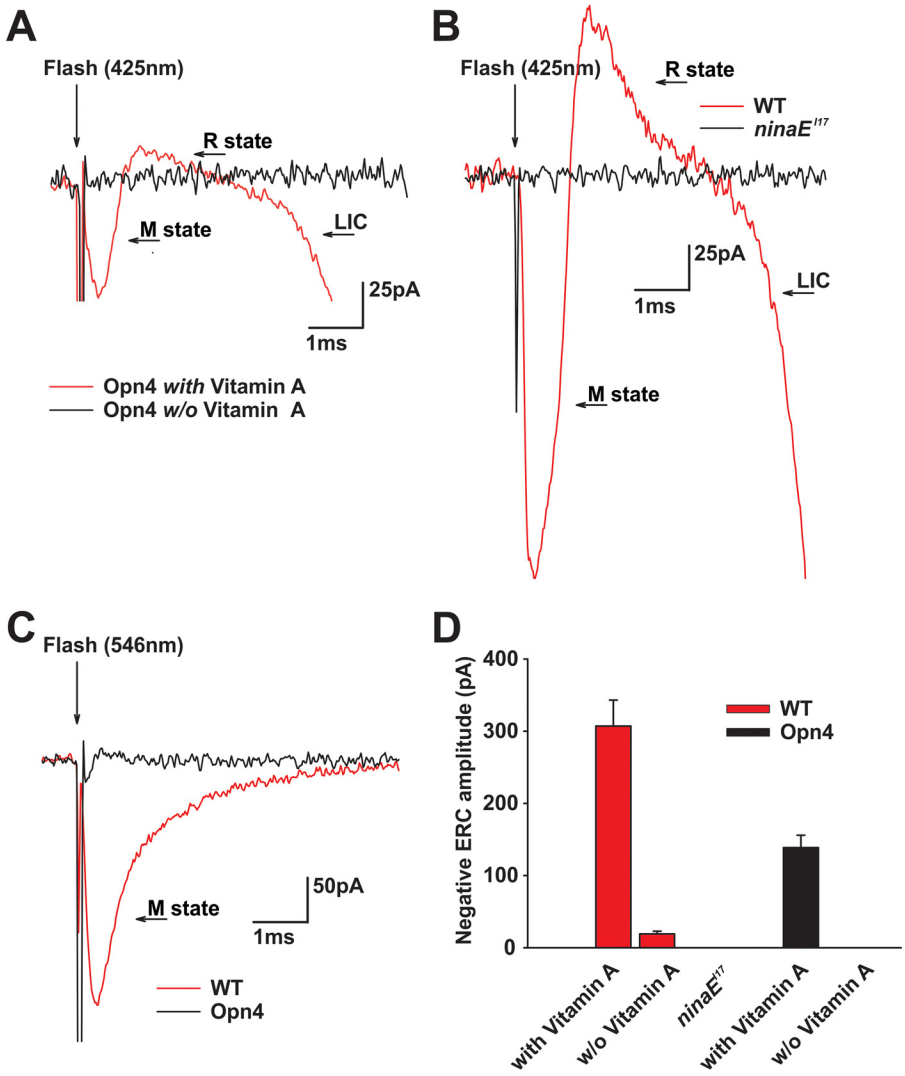

FIGURE 3. **ERC measurement of OPN4 and Rh1 photopigments.** *A*, ERC with biphasic waveform was recorded from *opn4;ninaE*^{I17} flies in response to blue light. Biphasic response with submicrosecond latency was recorded from isolated ommatidium of an *opn4;ninaE*^{I17} transgenic fly in response to intense 0.8-ms blue (broad band filter with peak absorption at 425 nm) flash stimulation applied after strong adaptation to orange (broad band filter with peak absorption at 546 nm) light (*red trace*). The flash onset is indicated by the *arrow*. A fast electrical artifact is also observed in all traces at light onset. The second (delayed) negative phase of this response arises from activation of LIC due to openings of the light-sensitive channels. The *black trace* shows a lack of ERC response to the same light flash applied to isolated ommatidium of *opn4;ninaE*^{I17} transgenic flies raised on retinoid-deficient medium. *B*, ERC with biphasic waveform but of larger amplitude is recorded from WT fly in response to blue light. Biphasic ERC response was recorded from isolated ommatidium of white-eyed WT fly in response to the same blue stimulation as in *A* after strong adaptation to the same orange light (*red trace*). The *black trace* shows a lack of any response to the same flash light recorded from isolated ommatidium of the *ninaE*^{I17} mutant. *C*, biphasic ERC with small amplitude is recorded from *opn4;ninaE*^{I17} flies in response to orange light. *Black trace*, biphasic small ERC response of isolated *opn4;ninaE*^{I17} photoreceptors to orange flash stimulus after strong adaptation to the blue (425 nm) light. *Red trace*, monophasic negative response to orange stimulation of WT fly after strong adaptation to blue light. Note the change in current scale between *A* and *B* relative to *C*. *D*, histograms plotting the averaged peak ERC negative amplitude of WT and *opn4;ninaE*^{I17} flies under various conditions. The peak amplitudes of the average negative ERC amplitudes of WT and *opn4;ninaE*^{I17} flies are shown for flies raised on medium with or without (*w/o*) vitamin A supplementation to the deficient medium. A lack of any ERC response in *ninaE*^{I17} mutants is also shown (*error bars*, S.E.; $n = 8$).

Fig. 3*C*, *black trace*) and elicited only small responses to green-orange light (Fig. 3*C*, *black trace*), suggesting largely overlapping R and M blue spectra. Thus, the measured ERC action spectra of the positive (Figs. 3*A* and 5, *bottom*, *blue*) and negative ERC (Figs. 3*A* and 5, *bottom*, *red*) phases of *opn4;ninaE*^{I17} flies were strikingly different from those of WT flies, although both were measured under identical conditions. The OPN4 action spectra showed a broadened blue spectra for both negative and positive ERCs, which were wider than a Dartnall nomogram that represents the absorption spectrum of a single pigment state (Fig. 5, *bottom*, *black curve*; also see "Discussion"). The broadened blue action spectrum is reminiscent of the recently published combined action spectra of mouse OPN4 pigment states, supporting our suggestion that the ERC of *opn4;ninaE*^{I17} photoreceptor cells reflects expression of mouse OPN4 in fly R1–6 photoreceptor cells (see Ref. 5 and "Discussion").

The Light Response of Opn4-expressing Drosophila Photoreceptors Is Much Faster than the Light Response of ipRGC—The slow physiological light response of ipRGC expressing the native melanopsin has been attributed to an intrinsic property of melanopsin (25). In contrast to the slow light response of ipRGC, the light response of fly photoreceptors is very fast (*e.g.* see Ref. 42). The light-induced current (LIC) of WT flies can be

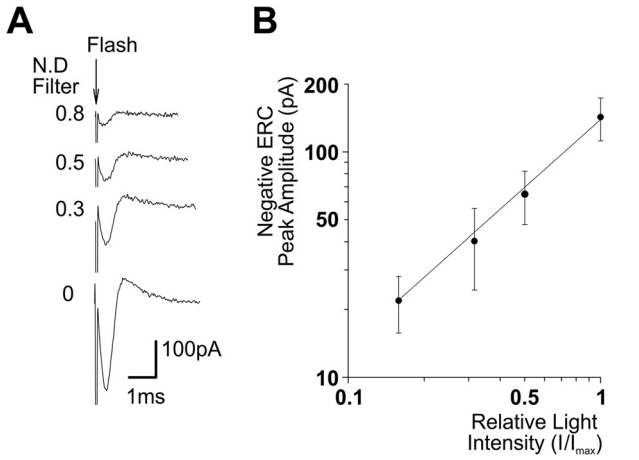

FIGURE 4. **The ERC amplitude increases linearly with the increase in light intensity.** *A*, ERCs with biphasic waveform were recorded from *opn4;ninaE*^{I17} flies in response to increasing intensities of white flash lights. Shown are a sample of ERC traces measured from a single cell of *opn4;ninaE*^{I17} in response to increasing intensities of white flash lights of different intensities (in relative −log *I* scale; *N.D.*, neutral density filters). The flash onset is indicated by the *arrow*. *B*, intensity-response relationship of the ERC measured in Opn4-expressing flies. The average peak amplitudes of the negative phase of ERC responses are plotted as a function of relative log light intensity (I/I_{max}, in log scale). The *continuous straight line* represents a linear regression curve that best fits the experimental points ($R^2 = 0.99$; *error bars*, S.E.; $n = 5$).

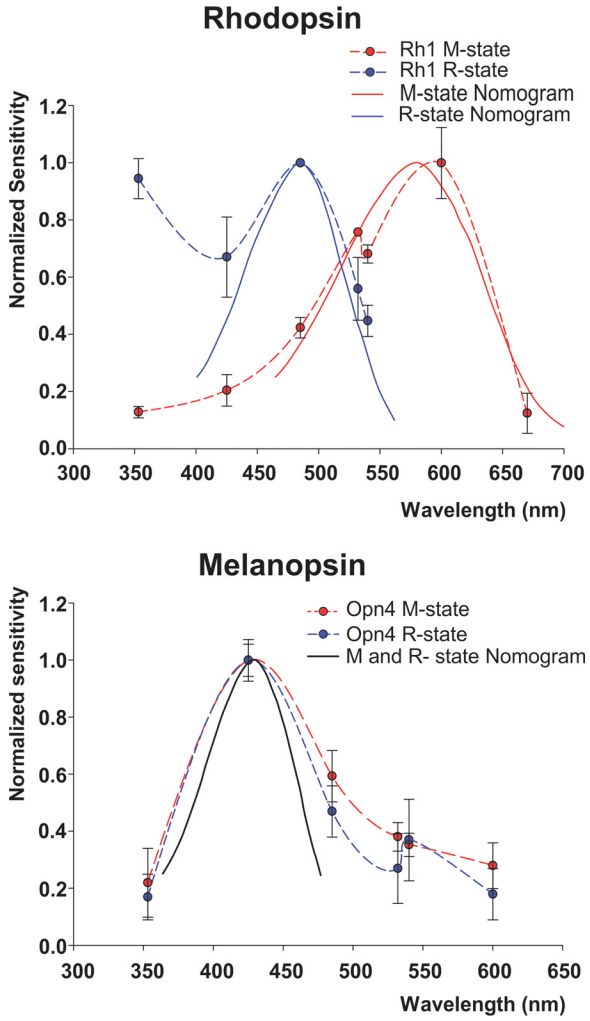

FIGURE 5. **Action spectra of the R and M photopigment states of mouse OPN4 and *Drosophila* Rh1 photopigments calculated from ERC measurements.** *Top*, experiments showing the well known action spectra of *Drosophila* Rh1 R and M pigment states as measured by the ERC. The normalized sensitivity, the reciprocal of the relative number of photons required to elicit a criterion ERC, is plotted on a linear scale against stimulus wavelength. The *blue* and *red dots* were measured from the peak amplitudes of the positive ERC (R state) and negative ERC (M state), respectively, both measured by whole cell recordings. The entire spectrum was measured from single R1–6 photoreceptor cells of white-eyed WT flies, and the spectrum represents the average calculation from different cells. For measuring the R state, the ommatidia were first orange-adapted, and then a test flash of specific peak wavelengths (broad band *colored filters*; see Table 1) elicited the measured positive ERC. This procedure was repeated for each point of the R spectrum. Then the ommatidia were blue-adapted, and the same procedure was used to measure the spectrum of the negative ERC (M state). The *smooth curves* are Dartnall nomograms having typical shapes of photopigment spectrum peaking at 485 nm (*blue*) and 580 nm (*red*). The increased sensitivity of the R state at the UV range is typical for the absorption of the fly UV-sensitizing pigment (41) (*error bars*, S.E.; $n = 8$). *Bottom*, action spectra of the expressed mouse OPN4 11-*cis* and 7-*cis* (*R*) and all-*trans* (*M*) states. The action spectra of mouse OPN4 R (positive ERC; *blue*) and M (negative ERC; *red*) states were measured in an identical way and in the same setup and filters (but see below) used for *Drosophila* Rh1 photopigment. Because the shape of the ERC elicited from *opn4;ninaE*^{I17} photoreceptors did not change with color adaptation, most measurements were performed after green adaptation, and some were verified using blue and orange light adaptation. The *smooth black curve* is a Dartnall nomogram peaking at 433 nm (*error bars*, S.E.; $n = 16$).

elicited by a wide range of light intensities. The LIC during dim lights is composed of unitary responses to absorption of single photons (quantum bumps) of ~13-pA averaged amplitude, whereas the LIC during intense lights can reach a peak amplitude of >15 nA, when the light intensity is increased by 5 orders of magnitude (42). Surprisingly, intense lights that elicit LIC of ~15-nA currents in WT flies were not sufficiently intense to elicit LIC in *opn4;ninaE*^{I17} flies. An unattenuated 150-J xenon light flash or an unattenuated continuous xenon light pulse that elicits >20 nA LIC in WT was required to elicit relatively small amplitude LICs with unusual properties in *opn4;ninaE*^{I17} flies (Fig. 6*A*). These LICs of *opn4;ninaE*^{I17} flies revealed highly variable amplitudes and variable durations after light off (Fig. 6*D*).

Despite the huge difference between the sensitivity to light of *opn4;ninaE*^{I17} and WT flies, the kinetics of their LIC was fast, much faster than the LIC kinetics of the ipRGC (Fig. 7). A comparison of the LIC waveform and time to peak of *opn4;ninaE*^{I17} photoreceptors and ipRGC obtained from a previous study (5) revealed a striking difference in their kinetics (Fig. 7). The time to peak of the flash response of ipRGC was ~40-fold slower than this parameters measured in *opn4;ninaE*^{I17} photoreceptors (Fig. 7).

Light-induced Production of Unitary Currents in the Dark in Opn4-expressing Drosophila Photoreceptors—The LICs of *opn4;ninaE*^{I17} photoreceptors were composed of observable unitary currents, reminiscent of WT quantum bumps, and they appeared long after light off (Fig. 6, *A*, *C*, and *D*). Despite the extremely intense light stimuli used for eliciting these responses, the maximal currents observed in *opn4;ninaE*^{I17} photoreceptor cells were usually in the subnanoampere range (Fig. 6*D*). In some cells, no LIC was elicited, despite the generation of an ERC. Thus, the LIC of *opn4;ninaE*^{I17} photoreceptor cells differed from that of WT photoreceptors in two main features: (i) they were insensitive to light, so that extremely intense lights induced unitary currents similar in shape to single photon responses, which are observed in WT flies only during extremely dim lights (~9 orders of magnitude dimmer than those used for *opn4;ninaE*^{I17} photoreceptor); (ii) they showed

TABLE 1
Properties of used filters

Filter	Peak wavelength	Full width at half-height	Relative transmittance
	nm	*nm*	*%*
UV	357	53	96
Blue	425	43	96
Blue-green	480	90	48
Green1	540	34	100
Green2	546	33	93
Red	673	40	86
Orange	Long pass edge	590 (at 50% transmission)	80

continuous production of quantum bump-like unitary currents, which were observed long (*e.g.* ~90 s) after light off, even when white light was applied (see below; see Fig. 6*C*).

To explore the similarity between the intense light-induced unitary currents of *opn4*;*ninaE*^{I17} photoreceptors and the quantum bumps of WT flies, we compared the bump amplitude distribution of the two fly strains (Fig. 8). The quantum bumps are known to have a stereotypic, rather uniform, shape but wide distribution of peak amplitudes (43). Therefore, the histogram of bump amplitude distribution is a useful tool to characterize the bumps (43). The bump amplitude distribution of the two fly strains was significantly different. In WT flies, the bump amplitude distribution fit well a normal distribution, whereas that of *opn4*;*ninaE*^{I17} photoreceptors did not fit well a normal distribution but showed a wider amplitude distribution with a smaller maximum. It included large fraction of abnormally small bumps, typical for *Drosophila* $G_q\alpha$ mutant with very low $G_q\alpha$ concentration (44). It also included a fraction of larger bumps that may represent the summation of 2–3 smaller bumps (Fig. 7*B*). Accordingly, the histogram presenting the averaged peak bump current of WT and *opn4*;*ninaE*^{I17} photoreceptors (Fig. 7*B*, *inset*) showed statistically significant difference between the mean bump amplitudes of the two fly strains (see "Discussion").

Induction of a PDA in opn4;ninaE^{I17} *Photoreceptors*—In a typical bistable pigment system, in which a large spectral overlap exists between the R and M photopigment states (*e.g.* in the *Limulus* (45)), a relatively small net amount of photopigment molecules can be shifted from one dark stable pigment state to the other. In contrast, in a tristable photopigment system, even when large spectral overlap exists between the photopigment 11-*cis* and all-*trans* states, a considerable amount of photopigment can be shifted between the 11-*cis* and all-*trans* pigment states (5, 46). In *opn4*;*ninaE*^{I17} photoreceptors, when maximal intensity blue (~430 nm) light was applied to dark-raised *opn4*;*ninaE*^{I17} flies, in some cells with relatively large peak LIC amplitude, the blue illuminated cells maintained their current response to the blue light, long after light off (Fig. 6*B*). Interestingly, the sustained current could be suppressed to baseline by a following intense green (~507-nm) light (Fig. 6*B*). This phenomenon is reminiscent of the prolonged depolarizing afterpotential (PDA (47); see "Discussion"). In contrast to the blue-green illumination paradigm, which most likely led to a net photopigment conversion (15), illumination with white light is not expected to cause a net photopigment conversion between the R and M states, which is required for induction and suppression of a PDA (47). Therefore, it is unlikely that the prolonged appearance in the dark of high frequency bumps, in response to intense white light, is a PDA (Fig. 6*C*). This notion was strongly supported by the application of intense orange light following the application of intense white light. This orange light induced an additional small amplitude noisy LIC during the light that did not suppress the prolonged appearance of bumps in the dark (Fig. 6, compare *B* and *C*). Thus, the ability to produce a PDA in *opn4*;*ninaE*^{I17} photoreceptors supports the recently demonstrated tristability of the native OPN4 of the ipRGC (5, 46).

Discussion

A Large Amount of OPN4 Was Ectopically Expressed in the Plasma Membrane of Drosophila Photoreceptor Cells—The scarcity of ipRGC and the low expression levels of phototransduction proteins in these cells make it difficult to investigate phototransduction of the ipRGC. The fact that several features of ipRGC photosensitivity are also characteristic of *Drosophila* photoreceptors (13) makes it possible to express large amounts of OPN4 in *Drosophila* photoreceptors and exploit the power of *Drosophila* genetics for investigating phototransduction of ipRGC. A powerful method to compare the functional similarity between melanopsin and the major fly photopigment, Rh1, is to replace *Drosophila* Rh1 with mouse OPN4 in the living fly. This can be done by generating transgenic flies, which express OPN4 in R1–6 photoreceptor cells in which Rh1 is eliminated. Measurements of RT-PCR, immunocytochemical localization of OPN4 to the base of the rhabdomeres, and the partial rescue of rhabdomeral degeneration indicated expression of OPN4 in R1–6 cells (Figs. 1 and 2).

In the *opn4*;*ninaE*^{I17} flies, a minor fraction of the recorded cells did not induce LIC, whereas a major fraction gave only small responses to extremely intense lights (Fig. 6*D*). These observations explain the reason for the lack of light response in the *opn4*;*ninaE*^{I17} flies in previous studies, which used the insensitive ERG measurement (23). Because whole cell recordings showed small but detectable responses to light in R1–6 photoreceptors of the transgenic fly, we used the ERC signal to measure OPN4 expression level in the plasma membrane of single cells. Although the ERC is a physiological epiphenomenon, it is a reliable and useful tool for measuring photopigment expression in the surface membrane of individual photoreceptor cells. The ERC is a linear signal without amplification (35) (see Fig. 4), and thus activation of millions photopigment molecules in single cells is required for detecting a measurable ERC, which is larger than the noise (48). Indeed, the intense xenon flash, which activates all of the $\sim 4 \times 10^7$ Rh1 molecules of a single WT cell within 1 ms (Fig. 3, *B* and *D*), also elicited a sufficiently large ERC in the *opn4*;*ninaE*^{I17} photoreceptor cells that was readily distinguished from the noise (Fig. 3, *A* and *D*). The appearance of an ERC signal in *opn4*;*ninaE*^{I17} photoreceptors suggests a large OPN4 expression in the surface membrane of these cells.

Strong evidence that the measured ERC in *opn4*;*ninaE*^{I17} photoreceptor cells reflects light activation of OPN4 came from measurements of its action spectrum. The need to apply extremely intense color lights to elicit an ERC dictated the use of relatively broad band color filters. Therefore, the accuracy of

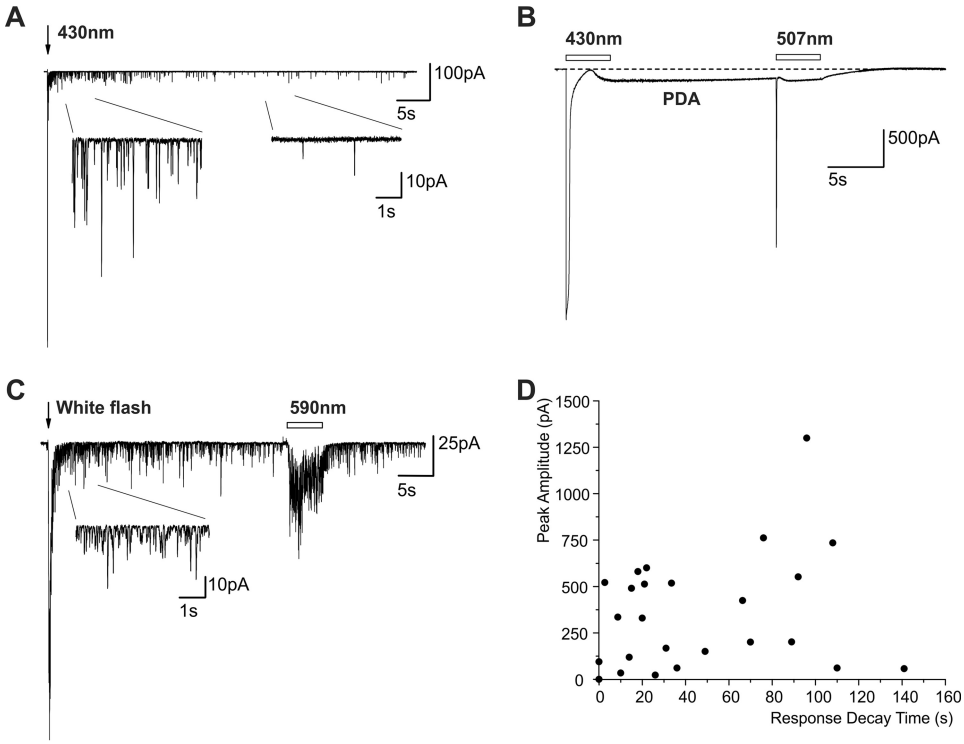

FIGURE 6. **The LIC of *opn4;ninaE^{I17}* transgenic flies.** *A*, the LIC induced by intense light is composed of unitary events similar to quantum bumps that appeared many seconds after light off. Whole cell recordings from a single R1–6 cell of *opn4;ninaE^{I17}* transgenic flies in response to intense blue (430-nm) flash light show slow response termination composed of quantum bumps. *Inset*, the LIC is composed of quantum bumps. The current fluctuations have roughly the shape and amplitudes of quantum bumps (as revealed in magnified scale; see Fig. 8). *B*, induction and suppression of a PDA in R1–6 cells of *opn4;ninaE^{I17}* transgenic flies. An intense long blue light pulse (*empty bar*) applied to dark-reared flies, which converted the 7-*cis* and 11-*cis* OPN4 pigment states to the all-*trans* M state, resulted in a PDA that continued in the dark. The following green light, which converted the all-*trans* OPN4 M state back to the original 11-*cis* states, suppressed the PDA. *C*, the prolonged appearance of quantum bumps in the dark after white light stimulation is not due to induction of a PDA because it could not be suppressed by orange light. The appearance of unitary currents similar to single photon responses in the dark (quantum bumps, *inset*) following application of white light could not be suppressed by an orange light pulse. *D*, a large variability in the LIC peak amplitude of the of *opn4;ninaE^{I17}* transgenic flies and a large variability in the duration of bumps appearance in the dark. The peak amplitudes of the LIC recorded from different cells is plotted as a function of the response decay time (the time of quantum bump disappearance) after application of flash light in the same individual cells.

the peak action spectra is limited. Nevertheless, a comparison of the OPN4 action spectra with the well characterized Rh1 action spectra revealed a substantial difference between the action spectra of the two photopigments, supporting the use of ERC as a reliable measure of photopigment properties. The main observed differences between Rh1 and OPN4 spectra were as follows. (i) The Rh1 R (3OH-11-*cis*) state revealed a dual UV and blue-green sensitivities, whereas OPN4 revealed a single blue peak. (ii) The Rh1 photopigment showed a wide separation between the action spectra of the R and M states, whereas the OPN4 R and M spectra largely overlap, as reported previously (Fig. 5). These observations are consistent with a recent study showing a detailed spectrophotometric characterization of purified mouse melanopsin as a tristable photopigment system, in which illumination with visible light produces a photo-steady state among three pigment states: 11-*cis*-melanopsin (peak absorption at 467 nm); all-*trans*-dark stable intermediate, *meta*-melanopsin (peak absorption at 476 nm); and the 7-*cis* state called extramelanopsin (peak absorption at 446 nm (15)). The mixture of these three pigment states gave a broadened blue action spectrum in ipRGC M1 cells, which was wider than the spectrum of any single pigment state (5). The prevailing view is that 7-*cis* photopigments are disfavored in nature (49). Nevertheless, two recent studies attributed an important functional role to the 7-*cis* isomer of OPN4 (5, 46). The detailed spectrophotometric measurements of mouse OPN4 (15) indicate that the ERC-positive phase of Fig. 3*A* (>530-nm adaptation and 425-nm flash stimulation) arises mainly from activation of the 7-*cis* pigment state. To the best of our knowledge, this is the first observation of an ERC from activation of a 7-*cis* photopigment.

The averaged negative ERC peak amplitude, arising from activation of the Rh1 M state of WT flies was 2.21-fold larger than the averaged negative ERC peak amplitude of OPN4-expressing flies. Assuming that the averaged maximal WT ERC amplitude reflects synchronous activation of $\sim 4 \times 10^7$ Rh1 molecules (assuming 4×10^4 microvilli in each cell and 10^3 Rh1 molecules in each microvillus (50)), the average maximal negative OPN4 ERC reflects activation of $\sim 1.9 \times 10^7$ OPN4 molecules. The ERC data thus indicates that a large amount of OPN4 is expressed in the photoreceptors' surface membrane of *opn4*; *ninaE^{I17}* transgenic flies.

Limited Functional Expression of OPN4 in Drosophila Ommatidia—A striking observation found in the OPN4-expressing flies was that extremely intense white (or blue) lights were required to elicit a relatively small LIC composed of single photon responses. This observation can be explained in several ways: (i) by the very small expression level of OPN4 in *opn4*; *ninaE^{I17}* photoreceptor cells; (ii) by inefficient coupling between OPN4 and the fly G_q protein; or (iii) by assuming that

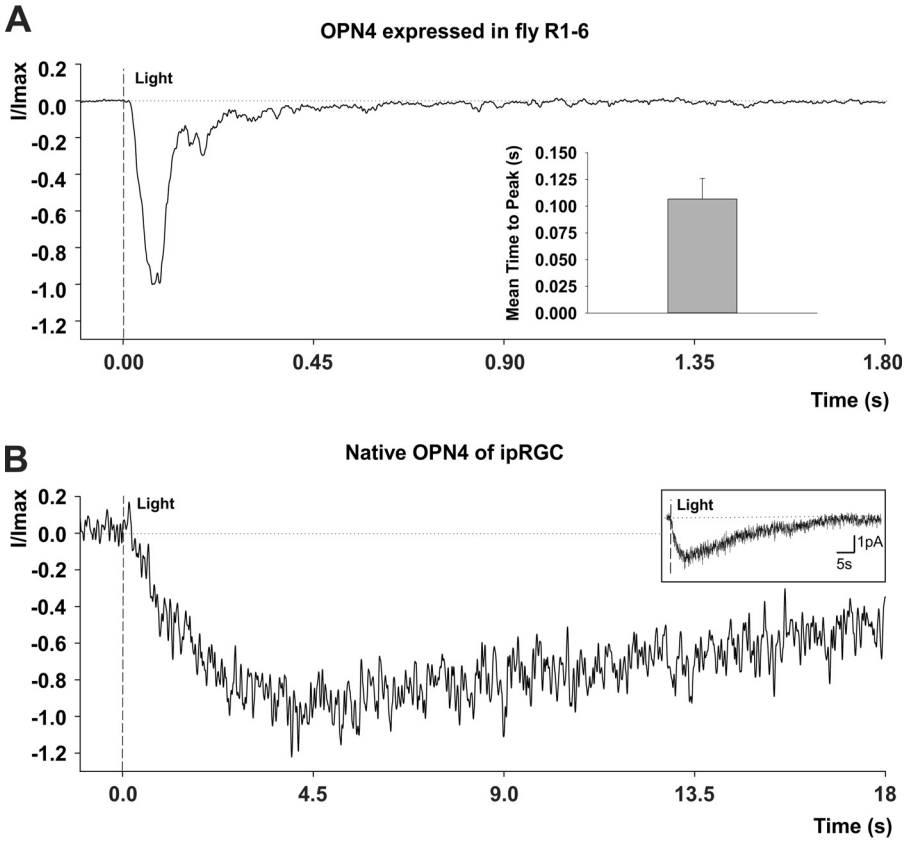

FIGURE 7. **A comparison of the kinetics of LIC of *opn4;ninaE^{I17}* transgenic flies and the ipRGC of mice.** *A*, normalized LIC of *opn4;ninaE^{I17}* transgenic flies. Whole cell recordings from a single R1–6 cell of *opn4;ninaE^{I17}* transgenic flies in response to intense white flash light showing the normalized typical shape of its LIC. *Inset*, a histogram of the averaged time to peak (from light onset) of the LICs of *opn4;ninaE^{I17}* photoreceptors. *Error bar*, S.E. ($n = 10$). *B*, normalized LIC of ipRGC of a mouse. LIC recorded from ipRGC of a mouse using a perforated patch recording. The flash is at time 0 and delivered 2.95×10^6 photons/μm^2 (480 nm, 50 ms, covering the somatodendritic compartment). The response is in the linear range of the dark-adapted cell, at room temperature (~23 °C). Each sweep is filtered at 10 Hz and sampled at 100 Hz; the average normalized LIC is of 14 trials. *Inset*, the trace of the main figure, presented in an extended time and current scale. (unpublished results from Emanuel and Do (5) with permission of the authors).

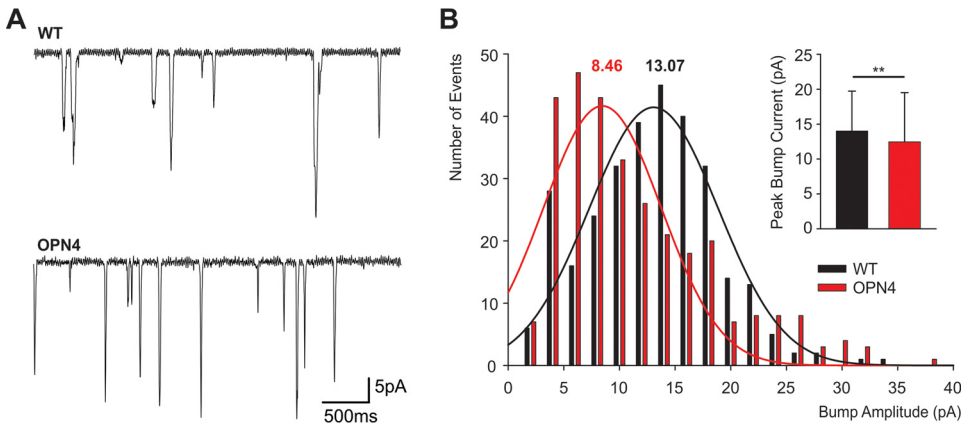

FIGURE 8. **A comparison between light induced unitary current events of WT and *opn4;ninaE^{I17}* transgenic flies.** *A*, single photon responses (quantum bumps) of WT fly (*top*) and unitary current events of *opn4;ninaE^{I17}* transgenic flies (*bottom*). *Top*, a representative sample of quantum bumps obtained from WT photoreceptor during dim orange light stimulation arising from xenon light source with maximal intensity attenuated to obtain frequency of 1.5 bumps/s. *Bottom*, representative samples of unitary currents obtained from *opn4;ninaE^{I17}* photoreceptor in the dark after application of maximal intensity white flash. *B*, a comparison of bump amplitude distribution between *opn4;ninaE^{I17}* (*red*) and WT flies (*black*). The histograms plot the number of bump events as a function of peak bump amplitude. The smooth curves are Gaussian distributions that best fit the experimental data. The *numbers above* the *curves* are the values of the peak Gaussian distributions. Note that the Gaussian distribution fits well the amplitude distribution of WT but not of *opn4;ninaE^{I17}* bumps. *Inset*, histogram plotting the averaged peak amplitudes of the bump currents of *opn4;ninaE^{I17}* (*red*) and WT flies (*black*). *Error bars*, S.D. 300 bumps were used for the analyses of each fly strain. The difference between *opn4;ninaE^{I17}* and WT flies is significant (*t* test, $p < 0.01$).

only a small fraction of the expressed OPN4 molecules reached the microvillar rhabdomeric membrane, allowing activation of only a small fraction of G_q molecules. The ERC measurements implicated large OPN4 expression at the surface membrane. However, the immunocytochemical localization of OPN4, mainly to the rhabdomeral stalk, strongly suggests that the rel-

atively small LIC amplitudes in these transgenic flies in response to intense lights are due to low expression levels of OPN4 in the signaling compartment where the G_q molecules reside. The large variability in LIC amplitudes of *opn4*;*ninaE*^{I17} photoreceptor cells is consistent with the sporadic immunocytochemical localization of OPN4 to the base of the rhabdomeres. It is unlikely that this variability arises from fluctuations in the total OPN4 expression levels because there were relatively small fluctuations in ERC amplitude, which reflect the total OPN4 expression levels.

Although the sequence homology between *Drosophila* $G_q\alpha$ and the various mammalian $G_q\alpha$ is high, they may not be sufficiently similar for efficient coupling between the mouse OPN4 and *Drosophila* $G_q\alpha$. Thus, an inefficient coupling between OPN4 and the *Drosophila* $G_q\alpha$ may also account for the induction of a small amplitude LIC composed of small quantum bumps in response to extremely intense light applied to the *opn4*;*ninaE*^{I17} photoreceptors. In addition, previous studies have shown that production of a quantum bump requires that a single active rhodopsin would activate 3–5 G_q molecules (42). This requirement predicts that inefficient coupling between OPN4 and *Drosophila* $G_q\alpha$ would induce abnormally small bumps, as was actually observed in strong $G_q\alpha$ mutants (42, 50, 51). This prediction fits with our observations that smaller bumps were observed in *opn4*;*ninaE*^{I17} photoreceptor cells (Fig. 8*B*), suggesting that inefficient coupling between OPN4 and fly $G_q\alpha$ may also contribute to the small LIC of *opn4*;*ninaE*^{I17}. The above considerations and the immunocytochemical localization of OPN4 strongly suggest that the major cause for the small LIC of *opn4*;*ninaE*^{I17} flies is the small fraction of expressed OPN4 molecules that reach the signaling compartment. Localization of OPN4 to the microvillar membrane is necessary for function. Only the small fraction of OPN4 molecules that reached the microvilli allow activation of the native G_q molecules.

A second striking observation of this study is the slow termination of the light response in *opn4*;*ninaE*^{I17}. This was manifested by quantum bump responses that were produced long after light off, whereas in WT flies, the quantum bumps appear only during dim illumination. This observation is best explained by an inefficient coupling between the active OPN4 in its all-*trans* M state and fly arrestin2. It was well established that fly arrestin2 greatly differs from the more common mammalian β-arrestin by showing Ca^{2+}-dependent phosphorylation (52). The prolonged appearance of quantum bumps in *opn4*;*ninaE*^{I17} flies in the dark following application of intense short white light is thus explained by inefficient coupling between OPN4 and fly arrestin2. An efficient coupling between these proteins is required for fast inactivation of the active photopigment molecules. Indeed, *Drosophila* with mutations in arrestin2 revealed continuous production of quantum bumps in the dark (21, 53). An additional intriguing observation in *opn4*;*ninaE*^{I17} photoreceptor cells, which is related to the coupling between fly arrestin2 and OPN4, is PDA induction by intense blue light. Strong support for the existence of a PDA in OPN4-expressing cells came from the recent study of Emanuel and Do (5), who demonstrated induction and suppression of a low amplitude PDA in ipRGC by blue and orange lights, respectively, during red illumination. In WT *Drosophila*, at least 20% (of total photopigment) net conversion of 3OH-11-*cis*-Rh1 to its all-*trans* M state is required for PDA induction (54, 55). Due to the OPN4 large spectral overlap between the absorption spectra of the 11-*cis*, 7-*cis*, and all-*trans* M state (5), a much smaller fraction of photopigment is converted in the *opn4*;*ninaE*^{I17} relative to WT fly (see Fig. 5). In WT *Drosophila*, the induction of the PDA is explained by the ~5-fold larger amount of Rh1 relative to arrestin2, which binds to the active all-*trans* M state and prevents its interaction with the G_q protein. Thus, at large amounts of photopigment activation (>20% of total), there is no sufficient amount of arrestin2 molecules to inactivate all active M state photopigment molecules following intense blue illumination, resulting in continuous excitation in the dark (56–58). The appearance of a PDA in *opn4*;*ninaE*^{I17} photoreceptors despite the large overlap among its dark-stable pigment states further suggests that the *Drosophila* arrestin2 is unable to bind efficiently to the OPN4 all-*trans* M state, resulting in a PDA. The fact that a PDA is induced in the native ipRGC was explained by the tristability of OPN4 (5).

Conclusions

The relative small peak amplitude of the OPN4-induced LIC in response to intense light and its large variability (Fig. 6*D*) suggest that only a small fraction of the expressed OPN4 reached the base of the rhabdomere and activated the fly G_q protein. The continuous production of quantum bump-like responses in *opn4*;*ninaE*^{I17} photoreceptor cells and the large variability in response termination time (Fig. 6*D*) reflect an inefficient coupling between OPN4 and fly arrestin2. The absence of a correlation between peak current amplitude and the duration of response termination in the dark suggests that these are two independent phenomena.

One of the most important properties of the *opn4*;*ninaE*^{I17} response to light found in this study is its fast kinetics, as reflected in the short time to peak of the response to light, which is ~40-fold shorter than the time to peak of the ipRGC response to light (Fig. 7*B*) (5, 59). This difference in light response kinetics indicates that the slow response kinetics of ipRGC does not arise from intrinsic properties of OPN4 but rather from the kinetics of downstream processes. A likely candidate for a potentially slow downstream process is the coupling between $G_q\alpha$ and PLCβ. Fly phototransduction is the fastest known G-protein-mediated transduction system. This is because of the large amounts of G_q and PLCβ in the signaling compartment of a single photoreceptor (50) and the extremely short distances of diffusion between G_q and PLCβ molecules in the microvilli (21). Indeed, it was shown that a large specific reduction in PLCβ concentration of *Drosophila* photoreceptors dramatically slowed down the kinetics of the light response (60, 61). Thus, the coupling of ectopically expressed OPN4 with the native $G_q\alpha$ and PLCβ of fly photoreceptors generates an extremely fast phototransduction cascade, which can be very useful for investigating the still unclear mechanism of OPN4-activated phototransduction.

Experimental Procedures

Fly Stocks—White-eyed w^{1118} (WT), red-eyed Oregon R, $ninaE^{I17}$, and P[Rh1:OPN4];$ninaE^{I17}$ flies were raised at 24 °C in a 12-h dark/light cycle. For the whole cell recordings, flies were dark-reared for at least 24 h before eclosion. The P[Rh1:OPN4];$ninaE^{I17}$ flies were a kind gift from Craig Montell (23).

Retinoid Deprivation—To reduce the expression level of the OPN4 and Rh1 photopigments, we raised the transgenic flies under retinoid-deficient medium for 3 generations and WT flies for 1–2 generations. The medium contained 10 g of dry yeasts, 10 g of glucose, 12 g of rice powder, 2 g of methyl paraben, 2 g of agar boiled in 200 ml of H_2O, 0.8 ml of propionic acid, 60 mg of cholesterol, 240 ml of H_2O (38). To restore the photopigment expression, the flies were raised for 1 generation with the above medium supplemented with vitamin A.

Whole Cell Recordings—Whole cell recordings from fly photoreceptors were performed as described previously (9, 62). In short, dissociated ommatidia were prepared from newly eclosed flies (<4 h post-eclosion). Recordings were made at 21 °C using patch pipettes of 8–12-megaohm resistance, pulled from fiber-filled borosilicate glass capillaries. Junction potential was nulled before seal formation. Series resistance was carefully compensated (>80%) for currents >100 pA. Membrane potential was clamped to −70 mV. Signals were amplified using an Axopatch-1D (Molecular Devices, Sunnyvale, CA) patch clamp amplifier. Currents were sampled at 10 kHz using an A/D converter (Digidata 1320a), filtered at 5 kHz. Responses were analyzed offline using Clampfit version 10.2 software (Molecular Devices). The light source was a xenon high pressure lamp (Lambda LS, Sutter Instruments) combined with an orange filter (Schott OG590 edge filter) or a xenon flash lamp system (JML-C2, Dr. Rapp OptoElecftronic, Hamburg, Germany). The light was delivered to the ommatidia via the microscope's epi-illumination port to the objective lens and was attenuated by a series of neutral density filters (Chroma). The shutter (Lambda SmartShutter, Sutter Instruments) open duration was controlled by a pulse generator (Master 8, AMPI).

ERC Recordings and Measurements of Action Spectra—ERC recordings were performed using whole cell patch clamp recordings from single R1–6 cells as described above. The light source for eliciting the ERC was a xenon flash lamp system (JML-C2, Dr. Rapp OptoElecftronic). The flash lamp emitted a 150-J light flash of 0.8-ms duration into a quartz light guide. The emitted flash light was delivered to the ommatidia via the microscope's epi-illumination port through the objective lens. For measurements of action spectra, band pass interference-type broad band filters (Chroma; see Table 1) were used. The response amplitudes of the positive or negative peaks of the ERC were normalized by the filter total transmittance to achieve a constant quantum flux for all filters (32). This calculation can be done due to the linear nature of the ERC response (Fig. 4). To determine a constant quantum flux for all of the color filters used for measuring the action spectra, we measured the transmission of each filter at the various wavelengths by a spectrophotometer.

Electron Microscopy—The procedure for transmission electron microscopy was described previously (63). Briefly, flies were raised in complete darkness 24 h before hatching, and heads were separated and bisected longitudinally from newly eclosed flies. Fly heads were cut in half in the sagittal plane and incubated in fixative solution (5% glutaraldehyde, 0.1 M cacodylate buffer, pH 7.4) and incubated overnight. Samples were then post-fixed (1% OsO_4, 0.1 M cacodylate buffer, pH 7.4), dehydrated through a graded series of ethanol, and embedded in epoxy resin. Ultrathin sections were stained with uranyl acetate and lead citrate, observed with a Tecnai-12 transmission electron microscope (FEI), and photographed with a Mega-view II charge-coupled camera.

TABLE 2
Primers used

Primer name	Sequence
*Opn4*_f	5′-CAAGGCATTTGGAACGGCACTCAGA
*Opn4*_r	5′-AACTCGCAACCTGTCTCCCCAAAGA
*pinta*_f	5′-TTCGCCGACAGTCGTTACCGC
*pinta*_r	5′-CACTGCCGCCACACTAACCCC

RNA Isolation and RT-PCR—Total RNA was isolated by homogenizing 20 *Drosophila* heads in 800 μl of TRIzol reagent and centrifuged at 12,000 × *g* for 10 min at 4 °C. The supernatant was incubated with 160 μl of chloroform and centrifuged at 10,000 × *g* for 15 min at 4 °C. The aqueous phase was transferred to 400 μl of isopropyl alcohol and centrifuged at 12,000 × *g* for 10 min at 4 °C. The supernatant was removed, and the pellet was washed with ethanol. The concentration and purity of the RNA samples were determined using a spectrophotometer. 1 ng of total RNA was reverse transcribed using a Verso cDNA synthesis kit (Thermo Scientific) and the supplied oligo(dT) primer. PCR on the cDNA library was performed using Phusion high fidelity DNA polymerase (Finnzyme) and designed primers (Table 2).

Western Blotting Analysis—To detect the *Drosophila* eye signaling proteins, 10 dark raised, newly eclosed fly heads of P[Rh1:OPN4];$ninaE^{I17}$, WT, $ninaE^{I17}$, $Gq\alpha^{1}$, $norpA^{H44}$, trp^{343}, $trpl^{302}$ transgenic, and null or hypermorph mutant flies were homogenized in a buffer solution (25 mM Tris, 150 mM NaCl, 5 mM EDTA, 1% Triton X-100, protease inhibitor, pH 7.5) and centrifuged at 12,000 × *g* for 15 min at 4 °C. Laemmli buffer was added to the supernatant, which was boiled to 95 °C for 5 min and separated using 6–12% SDS-PAGE. Proteins were transferred for 1 h at 350 mA to BioTrace™ PVDF membranes (Pall Corp.) in Tris-glycine buffer supplemented with 20% methanol. The blots were probed by anti-Rh1 (monoclonal, 1:1,000 dilution; Developmental Studies Hybridoma Bank), anti-$G_q\alpha$ (polyclonal, 1:2,000; Dr. Z. Selinger), anti-PLCβ and anti-TRPL (polyclonal, 1:1,000; Dr. A. Huber), anti-TRP (monoclonal, 1:500; from Developmental Studies Hybridoma Bank), and anti-dMoesin (polyclonal, 1:10,000; Dr. F. Payre). Signals were detected using EZ-ECL reagents (Biological Industries). Relative protein amounts were quantified using ImageJ software (64). The density in each lane was corrected by the dMoesin signal (65) and calculated as a percentage of WT fly signals.

Immunocytochemistry of Fly Eyes—Freshly eclosed flies (< 1 day old) were used for the experiments. Immunocytochemistry of fly eyes was carried out as described previously (66) except that sections were additionally incubated after fixation on a shaker in 0.5% Triton X-100 in PBS (175 mM NaCl, 8 mM

Na_2HPO_4, and 1.8 mM NaH_2PO_4, pH 7.2) for 16 h to wash out a large amount of screening pigments present in the eyes of P[Rh1:OPN4];*ninaE*^{I17} and in the wild type (Oregon R) control flies. α-OPN4 (ThermoFisher (PA1-780)) was used as primary antibody. Secondary antibody was α-rabbit Cy5 (Dianova). Alexa Fluor 546-coupled phalloidin (Life Technologies, Inc.) was used to label the actin cytoskeleton of the rhabdomeres.

Author Contributions—B. Y. performed most of the electrophysiological experiments, prepared the figures, and analyzed the data. E. K. performed some of the electrophysiological experiments. S. W. performed the EM studies. R. Z. performed the Western blotting analysis and part of the RT-PCR. M. P. performed the RT-PCR. B. K. interpreted the data, prepared the final figures, and drafted and wrote the manuscript. A. H. and K. S. performed the immunocytochemistry, and B. M. designed the study, interpreted the data, and drafted and wrote the manuscript.

Acknowledgments—We thank Dr. Craig Montell for the P[Rh1:OPN4];ninaE^{I17} *flies and Dr. Michael Do for providing unpublished data derived from ipRGC that were used in Fig. 7B and for invaluable advice. We thank Dr. Moshe Parnas for critical reading of the manuscript. We also thank Dr. François Payre for the antibodies against dMoesin.*

References

1. Hatori, M., and Panda, S. (2010) The emerging roles of melanopsin in behavioral adaptation to light. *Trends Mol. Med.* **16,** 435–446
2. Provencio, I., Rodriguez, I. R., Jiang, G., Hayes, W. P., Moreira, E. F., and Rollag, M. D. (2000) A novel human opsin in the inner retina. *J. Neurosci.* **20,** 600–605
3. Berson, D. M., Dunn, F. A., and Takao, M. (2002) Phototransduction by retinal ganglion cells that set the circadian clock. *Science* **295,** 1070–1073
4. Hattar, S., Liao, H. W., Takao, M., Berson, D. M., and Yau, K. W. (2002) Melanopsin-containing retinal ganglion cells: architecture, projections, and intrinsic photosensitivity. *Science* **295,** 1065–1070
5. Emanuel, A. J., and Do, M. T. (2015) Melanopsin tristability for sustained and broadband phototransduction. *Neuron* **85,** 1043–1055
6. Sekaran, S., Foster, R. G., Lucas, R. J., and Hankins, M. W. (2003) Calcium imaging reveals a network of intrinsically light-sensitive inner-retinal neurons. *Curr. Biol.* **13,** 1290–1298
7. Hattar, S., Lucas, R. J., Mrosovsky, N., Thompson, S., Douglas, R. H., Hankins, M. W., Lem, J., Biel, M., Hofmann, F., Foster, R. G., and Yau, K. W. (2003) Melanopsin and rod-cone photoreceptive systems account for all major accessory visual functions in mice. *Nature* **424,** 76–81
8. Panda, S., Provencio, I., Tu, D. C., Pires, S. S., Rollag, M. D., Castrucci, A. M., Pletcher, M. T., Sato, T. K., Wiltshire, T., Andahazy, M., Kay, S. A., Van Gelder, R. N., and Hogenesch, J. B. (2003) Melanopsin is required for non-image-forming photic responses in blind mice. *Science* **301,** 525–527
9. Hardie, R. C., and Minke, B. (1992) The *trp* gene is essential for a light-activated Ca^{2+} channel in *Drosophila* photoreceptors. *Neuron* **8,** 643–651
10. Minke, B. (2010) The history of the *Drosophila* TRP channel: the birth of a new channel superfamily. *J. Neurogenet.* **24,** 216–233
11. Graham, D. M., Wong, K. Y., Shapiro, P., Frederick, C., Pattabiraman, K., and Berson, D. M. (2008) Melanopsin ganglion cells use a membrane-associated rhabdomeric phototransduction cascade. *J. Neurophysiol.* **99,** 2522–2532
12. Xue, H. H., Zhao, D. M., Suda, T., Uchida, C., Oda, T., Chida, K., Ichiyama, A., and Nakamura, H. (2000) Store depletion by caffeine/ryanodine activates capacitative Ca^{2+} entry in nonexcitable A549 cells. *J. Biochem.* **128,** 329–336
13. Xue, T., Do, M. T., Riccio, A., Jiang, Z., Hsieh, J., Wang, H. C., Merbs, S. L., Welsbie, D. S., Yoshioka, T., Weissgerber, P., Stolz, S., Flockerzi, V., Freichel, M., Simon, M. I., Clapham, D. E., and Yau, K. W. (2011) Melanopsin signalling in mammalian iris and retina. *Nature* **479,** 67–73
14. Walker, M. T., Brown, R. L., Cronin, T. W., and Robinson, P. R. (2008) Photochemistry of retinal chromophore in mouse melanopsin. *Proc. Natl. Acad. Sci. U.S.A.* **105,** 8861–8865
15. Matsuyama, T., Yamashita, T., Imamoto, Y., and Shichida, Y. (2012) Photochemical properties of mammalian melanopsin. *Biochemistry* **51,** 5454–5462
16. Sexton, T. J., Golczak, M., Palczewski, K., and Van Gelder, R. N. (2012) Melanopsin is highly resistant to light and chemical bleaching *in vivo*. *J. Biol. Chem.* **287,** 20888–20897
17. Koyanagi, M., Kubokawa, K., Tsukamoto, H., Shichida, Y., and Terakita, A. (2005) Cephalochordate melanopsin: evolutionary linkage between invertebrate visual cells and vertebrate photosensitive retinal ganglion cells. *Curr. Biol.* **15,** 1065–1069
18. Mure, L. S., Rieux, C., Hattar, S., and Cooper, H. M. (2007) Melanopsin-dependent nonvisual responses: evidence for photopigment bistability *in vivo*. *J. Biol. Rhythms* **22,** 411–424
19. Mure, L. S., Cornut, P. L., Rieux, C., Drouyer, E., Denis, P., Gronfier, C., and Cooper, H. M. (2009) Melanopsin bistability: a fly's eye technology in the human retina. *PLoS One* **4,** e5991
20. Melyan, Z., Tarttelin, E. E., Bellingham, J., Lucas, R. J., and Hankins, M. W. (2005) Addition of human melanopsin renders mammalian cells photoresponsive. *Nature* **433,** 741–745
21. Katz, B., and Minke, B. (2009) *Drosophila* photoreceptors and signaling mechanisms. *Front. Cell Neurosci.* **3,** 2
22. Yau, K. W., and Hardie, R. C. (2009) Phototransduction motifs and variations. *Cell* **139,** 246–264
23. Shen, W. L., Kwon, Y., Adegbola, A. A., Luo, J., Chess, A., and Montell, C. (2011) Function of rhodopsin in temperature discrimination in *Drosophila*. *Science* **331,** 1333–1336
24. Ahmad, S. T., Natochin, M., Barren, B., Artemyev, N. O., and O'Tousa, J. E. (2006) Heterologous expression of bovine rhodopsin in *Drosophila* photoreceptor cells. *Invest. Ophthalmol. Vis. Sci.* **47,** 3722–3728
25. Rinaldi, S., Melaccio, F., Gozem, S., Fanelli, F., and Olivucci, M. (2014) Comparison of the isomerization mechanisms of human melanopsin and invertebrate and vertebrate rhodopsins. *Proc. Natl. Acad. Sci. U.S.A.* **111,** 1714–1719
26. Spoida, K., Eickelbeck, D., Karapinar, R., Eckhardt, T., Mark, M. D., Jancke, D., Ehinger, B. V., König, P., Dalkara, D., Herlitze, S., and Masseck, O. A. (2016) Melanopsin variants as intrinsic optogenetic on and off switches for transient *versus* sustained activation of G protein pathways. *Curr. Biol.* **26,** 1206–1212
27. Tsukamoto, H., Kubo, Y., Farrens, D. L., Koyanagi, M., Terakita, A., and Furutani, Y. (2015) Retinal attachment instability is dversified among mammalian melanopsins. *J. Biol. Chem.* **290,** 27176–27187
28. Ferrer, C., Malagón, G., Gomez Mdel, P., and Nasi, E. (2012) Dissecting the determinants of light sensitivity in amphioxus microvillar photoreceptors: possible evolutionary implications for melanopsin signaling. *J. Neurosci.* **32,** 17977–17987
29. Borges, R., Johnson, W. E., O'Brien, S. J., Vasconcelos, V., and Antunes, A. (2012) The role of gene duplication and unconstrained selective pressures in the melanopsin gene family evolution and vertebrate circadian rhythm regulation. *PLoS One* **7,** e52413
30. Pinal, N., and Pichaud, F. (2011) Dynamin- and Rab5-dependent endocytosis is required to prevent *Drosophila* photoreceptor degeneration. *J. Cell Sci.* **124,** 1564–1570
31. Wang, T., and Montell, C. (2005) Rhodopsin formation in *Drosophila* is dependent on the PINTA retinoid-binding protein. *J. Neurosci.* **25,** 5187–5194
32. Minke, B., Hochstein, S., and Hillman, P. (1973) Early receptor potential evidence for the existence of two thermally stable states in the barnacle visual pigment. *J. Gen. Physiol.* **62,** 87–104
33. Hardie, R. C. (1995) Photolysis of caged Ca^{2+} facilitates and inactivates but does not directly excite light-sensitive channels in *Drosophila* photoreceptors. *J. Neurosci.* **15,** 889–902
34. Cone, R. A. (1964) Early receptor potential of the vertebrate retina. *Nature* **204,** 736–739

35. Minke, B., Hochstein, S., and Hillman, P. (1974) Derivation of a quantitative kinetic model for a visual pigment from observations of early receptor potential. *Biophys. J.* **14,** 490–512
36. Harris, W. A., Ready, D. F., Lipson, E. D., Hudspeth, A. J., and Stark, W. S. (1977) Vitamin A deprivation and *Drosophila* photopigments. *Nature* **266,** 648–650
37. Isono, K., Tanimura, T., Oda, Y., and Tsukahara, Y. (1988) Dependency on light and vitamin A derivatives of the biogenesis of 3-hydroxyretinal and visual pigment in the compound eyes of *Drosophila melanogaster*. *J. Gen. Physiol.* **92,** 587–600
38. Wang, X., Wang, T., Jiao, Y., von Lintig, J., Montell, C. (2010) Requirement for an enzymatic visual cycle in *Drosophila*. *Curr. Biol.* **20,** 93–102
39. Pak, W. L., and Lidington, K. J. (1974) Fast electrical potential from a long-lived, long-wavelength photoproduct of fly visual pigment. *J. Gen. Physiol.* **63,** 740–756
40. Minke, B., and Selinger, Z. (1992) The inositol-lipid pathway is necessary for light excitation in fly photoreceptors. In *Sensory Transduction* (Corey, D., and Roper, S. D. eds) pp. 202–217, Rockefeller University Press, New York
41. Kirschfeld, K., Franceschini, N., and Minke, B. (1977) Evidence for a sensitising pigment in fly photoreceptors. *Nature* **269,** 386–390
42. Katz, B., and Minke, B. (2012) Phospholipase C-mediated suppression of dark noise enables single-photon detection in *Drosophila* photoreceptors. *J. Neurosci.* **32,** 2722–2733
43. Henderson, S. R., Reuss, H., and Hardie, R. C. (2000) Single photon responses in *Drosophila* photoreceptors and their regulation by Ca^{2+}. *J. Physiol. Lond.* **524,** 179–194
44. Scott, K., Becker, A., Sun, Y., Hardy, R., and Zuker, C. (1995) $G_q\alpha$ protein function *in vivo*: genetic dissection of its role in photoreceptor cell physiology. *Neuron* **15,** 919–927
45. Knox, B. E., Salcedo, E., Mathiesz, K., Schaefer, J., Chou, W. H., Chadwell, L. V., Smith, W. C., Britt, S. G., and Barlow, R. B. (2003) Heterologous expression of *Limulus* rhodopsin. *J. Biol. Chem.* **278,** 40493–40502
46. Mure, L. S., Hatori, M., Zhu, Q., Demas, J., Kim, I. M., Nayak, S. K., and Panda, S. (2016) Melanopsin-encoded response properties of intrinsically photosensitive retinal ganglion cells. *Neuron* **90,** 1016–1027
47. Minke, B. (2012) The history of the prolonged depolarizing afterpotential (PDA) and its role in genetic dissection of *Drosophila* phototransduction. *J. Neurogenet.* **26,** 106–117
48. Hillman, P., Dodge, F. A., Hochstein, S., Knight, B. W., and Minke, B. (1973) Rapid dark recovery of the invertebrate early receptor potential. *J. Gen. Physiol.* **62,** 77–86
49. Sekharan, S., and Morokuma, K. (2011) Why 11-*cis*-retinal? Why not 7-*cis*-, 9-*cis*-, or 13-*cis*-retinal in the eye? *J. Am. Chem. Soc.* **133,** 19052–19055
50. Frechter, S., Elia, N., Tzarfaty, V., Selinger, Z., and Minke, B. (2007) Translocation of $G_q\alpha$ mediates long-term adaptation in *Drosophila* photoreceptors. *J. Neurosci.* **27,** 5571–5583
51. Hardie, R. C., Martin, F., Cochrane, G. W., Juusola, M., Georgiev, P., and Raghu, P. (2002) Molecular basis of amplification in *Drosophila* phototransduction: roles for G protein, phospholipase C, and diacylglycerol kinase. *Neuron* **36,** 689–701
52. Matsumoto, H., and Yamada, T. (1991) Phosrestins I and II: arrestin homologs which undergo differential light-induced phosphorylation in the *Drosophila* photoreceptor *in vivo*. *Biochem. Biophys. Res. Commun.* **177,** 1306–1312
53. Liu, C. H., Satoh, A. K., Postma, M., Huang, J., Ready, D. F., and Hardie, R. C. (2008) Ca^{2+}-dependent metarhodopsin inactivation mediated by calmodulin and NINAC myosin III. *Neuron* **59,** 778–789
54. Hochstein S, Minke B, Hillman P. (1973) Antagonistic components of the late receptor potential in the barnacle photoreceptor arising from different stages of the pigment process. *J. Gen. Physiol.* **62,** 105–128
55. Hillman, P., Hochstein, S., and Minke, B. (1983) Transduction in invertebrate photoreceptors: role of pigment bistability. *Physiol. Rev.* **63,** 668–772
56. Byk, T., Bar-Yaacov, M., Doza, Y. N., Minke, B., and Selinger, Z. (1993) Regulatory arrestin cycle secures the fidelity and maintenance of the fly photoreceptor cell. *Proc. Natl. Acad. Sci. U.S.A.* **90,** 1907–1911
57. Selinger, Z., Doza, Y. N., and Minke, B. (1993) Mechanisms and genetics of photoreceptors desensitization in *Drosophila* flies. *Biochim. Biophys. Acta* **1179,** 283–299
58. Dolph, P. J., Ranganathan, R., Colley, N. J., Hardy, R. W., Socolich, M., and Zuker, C. S. (1993) Arrestin function in inactivation of G protein-coupled receptor rhodopsin *in vivo*. *Science* **260,** 1910–1916
59. Rollag, M. D., Berson, D. M., and Provencio, I. (2003) Melanopsin, ganglion-cell photoreceptors, and mammalian photoentrainment. *J. Biol. Rhythms* **18,** 227–234
60. Cook, B., Bar-Yaacov, M., Cohen Ben-Ami, H., Goldstein, R. E., Paroush, Z., Selinger, Z., and Minke, B. (2000) Phospholipase C and termination of G-protein-mediated signalling *in vivo*. *Nat. Cell Biol.* **2,** 296–301
61. Scott, K., and Zuker, C. S. (1998) Assembly of the *Drosophila* phototransduction cascade into a signalling complex shapes elementary responses. *Nature* **395,** 805–808
62. Peretz, A., Suss-Toby, E., Rom-Glas, A., Arnon, A., Payne, R., and Minke, B. (1994) The light response of *Drosophila* photoreceptors is accompanied by an increase in cellular calcium: effects of specific mutations. *Neuron* **12,** 1257–1267
63. Weiss, S., Kohn, E., Dadon, D., Katz, B., Peters, M., Lebendiker, M., Kosloff, M., Colley, N. J., and Minke, B. (2012) Compartmentalization and Ca^{2+} buffering are essential for prevention of light-induced retinal degeneration. *J. Neurosci.* **32,** 14696–14708
64. Schneider, C. A., Rasband, W. S., and Eliceiri, K. W. (2012) NIH Image to ImageJ: 25 years of image analysis. *Nat. Methods* **9,** 671–675
65. Chorna-Ornan, I., Tzarfaty, V., Ankri-Eliahoo, G., Joel-Almagor, T., Meyer, N. E., Huber, A., Payre, F., and Minke, B. (2005) Light-regulated interaction of Dmoesin with TRP and TRPL channels is required for maintenance of photoreceptors. *J. Cell Biol.* **171,** 143–152
66. Cerny, A. C., Altendorfer, A., Schopf, K., Baltner, K., Maag, N., Sehn, E., Wolfrum, U., and Huber, A. (2015) The GTP- and phospholipid-binding protein TTD14 regulates trafficking of the TRPL ion channel in *Drosophila* photoreceptor cells. *PLoS Genet.* **11,** e1005578
67. Scott, K., Sun, Y., Beckingham, K., and Zuker, C. S. (1997) Calmodulin regulation of *Drosophila* light-activated channels and receptor function mediates termination of the light response *in vivo*. *Cell* **91,** 375–383